PCCP

Alcohol dimers - how much diagonal OH anharmonicity?

Journal:	*Physical Chemistry Chemical Physics*
Manuscript ID:	CP-ART-04-2014-001418.R1
Article Type:	Paper
Date Submitted by the Author:	02-Jun-2014

Complete List of Authors:	Kollipost, Franz; Georg August Universitaet Goettingen, Institut fuer Physikalische Chemie Papendorf, Kim; Georg August Universitaet Goettingen, Institut fuer Physikalische Chemie Lee, Yu-Fang; National Chiao Tung University, Applied Chemistry Lee, Yuan-Pern; Institute of Atomic and Molecular Sciences, ; National Chiao Tung University, Department of Applied Chemistry and Institute of Molecular Science Suhm, Martin; Georg August Universitaet Goettingen, Institut fuer Physikalische Chemie

Alcohol dimers - how much diagonal OH anharmonicity?†

Franz Kollipost,[a] Kim Papendorf,[a] Yu-Fang Lee,[b] Yuan-Pern Lee[b,c] and Martin A. Suhm*[a]

Received Xth XXXXXXXXXX 20XX, Accepted Xth XXXXXXXXX 20XX
First published on the web Xth XXXXXXXXXX 200X
DOI: 10.1039/b000000x

The OH bond of methanol, ethanol and *t*-butyl alcohol becomes more anharmonic upon hydrogen bonding and the infrared intensity ratio between the overtone and the fundamental transition of the bridging OH stretching mode decreases drastically. FTIR spectroscopy of supersonic slit jet expansions allows to quantify these effects for isolated alcohol dimers, enabling a direct comparison to anharmonic vibrational predictions. The diagonal anharmonicity increase amounts to 15-18%, growing with increasing alkyl substitution. The overtone/fundamental IR intensity ratio, which is on the order of 0.1 or more for isolated alcohols, drops to 0.004-0.001 in the hydrogen-bonded OH group, making overtone detection very challenging. Again, alkyl substitution enhances the intensity suppression. Vibrational second order perturbation theory appears to capture these effects in a semiquantitative way. Harmonic quantum chemistry predictions for the hydrogen bond-induced OH stretching frequency shift (the widely used infrared signature of hydrogen bonding) are insufficient, and diagonal anharmonicity corrections from experiment make the agreement between theory and experiment worse. Inclusion of anharmonic cross terms between hydrogen bond modes and the OH stretching mode is thus essential, as is a high level electronic structure theory. The isolated molecule results are compared to matrix isolation data, complementing earlier studies in N_2 and Ar by the more weakly interacting Ne and *p*-H_2 matrices. Matrix effects on the hydrogen bond donor vibration are quantified.

1 Introduction

In 2006[1], the late Camille Sándorfy posed the general title question - hydrogen bonding: how much anharmonicity? Indeed, it is crucial to know how much the anharmonicity of an OH oscillator changes upon hydrogen bond formation. After all, the formation of a hydrogen bond may be viewed as a pre-reactive model for chemical bond breaking. It weakens the chemical bond of the donor, it lowers its vibrational frequency, and it does so by strengthening the link to the acceptor atom. In more reactive systems such as HCl, the bond can not be only softened[2], but ionically broken by adding a number of water molecules. The exact number of water molecules required is still under debate[3–5], from an experimental viewpoint. Here, we address a weaker perturbation in alcohol dimers, which nevertheless has remained somewhat in the dark[1]. Even without breaking the chemical bond, the coupling between the OH oscillator and the intermolecular vibrations controls the lifetime of molecular complexes after OH stretching excitation[6]. The question is also relevant for 2D time-resolved pump-probe IR experiments in condensed phase, which probe the anharmonicity by absorption out of the excited stretching fundamental level and would actually not work without this anharmonicity[7].

We concentrate on the diagonal anharmonicity constant $x_{\mathrm{OH,OH}}$, i.e. one half of the change in the OH stretching wavenumber upon previous excitation of the same OH stretching mode (to $v = 1$). In a one-dimensional Morse oscillator, it corresponds to $-\omega_e x_e$[8]. This constant can be determined in a straightforward way even in a polyatomic molecule by either measuring the above-mentioned hot transition or the overtone of the OH stretching fundamental. The former strategy is exploited in pump-probe schemes in the condensed phase[7], whereas the latter is the standard approach in gas phase[9] and matrix isolation measurements[10]. It suffers from a low IR intensity of the overtone, but profits from a high population of the ground state, at least in a cold supersonic jet expansion or matrix. This removes inhomogeneous broadening from low frequency excitations and ensures the required accuracy in determining the band center. Together with the absence of environmental perturbation in the case of jet spectroscopy, this experimental approach offers a perfect meeting point with anharmonic theory[11].

The position of an overtone transition is governed by the mechanical anharmonicity of the oscillator, but its intensity is controlled by both the mechanical anharmonicity and its elec-

† Electronic Supplementary Information (ESI) available: Computational results for methanol and ethanol monomers and dimers, compilation of experimental wavenumbers and absorbances. See DOI: 10.1039/b000000x/

[a] Georg-August-Universität Göttingen, Institut für Physikalische Chemie, Tammannstr. 6, 37077 Göttingen, Germany. Fax: +49 551 39 331117; E-mail: msuhm@gwdg.de
[b] Department of Applied Chemistry and Institute of Molecular Science, National Chiao Tung University, 1001 Ta-Hsueh Rd., Hsinchu 30010, Taiwan
[c] Institute of Atomic and Molecular Sciences, Academia Sinica, Taipei 10617, Taiwan

trical counterpart, namely a non-linear dipole moment curve along the oscillation[12]. Even for a perfectly harmonic oscillator, dipole moment curvature would induce infrared activity of the overtone transition. In an anharmonic potential, the two non-linear contributions may add to or partially cancel each other. Whenever an OH bond engages in a hydrogen bond, cancellation is typically dominant for the overtone intensity, whereas the fundamental transition profits enormously from the steepening of the dipole curve due to bond polarization. Instead of an order of magnitude drop in intensity from fundamental to overtone transitions in isolated OH bonds, two or more orders of magnitude may be expected for hydrogen-bonded OH groups[12]. Indeed, 8 decades ago, the absence of an OH stretching overtone has been used as evidence for hydrogen bonding[13]. This makes overtone detection technologically demanding, even more so at high gas phase dilution typical for supersonic jet expansions. Therefore, only the most sensitive jet spectrometers are capable of detecting these weak overtones in hydrogen-bonded dimers[11,14].

We choose simple alcohols as the test cases, because in contrast to water[15], they offer a single isolated hydride oscillator which is sufficiently decoupled from other intramolecular modes[16]. Their simplest symmetric representatives methanol and *t*-butyl alcohol are elementary enough to invite high level quantum chemical calculations of their dimers[17,18]. Ethanol is presented as a case where the oscillator strength is distributed among several dimer conformations[19], rendering detection even more challenging. The study of aliphatic alcohols precludes techniques which exploit UV/IR double resonance, except for the VUV variant which is susceptible to fragmentation dynamics[20] and therefore requires careful analysis[21] as well as femtosecond multiphoton ionization, which can lead to band broadening[22]. We use a non-selective FTIR absorption approach, which enables a direct comparison of fundamental and overtone excitation[11]. By pulsed expansion of alcohol-rare gas mixtures through a 600 mm long slit nozzle[23], sufficient absorption is achieved, when the infrared attenuation is detected with a sensitive detector.

Information on the OH stretching anharmonicity in such simple alcohol dimers was so far restricted to matrix isolation studies[10], where matrix shifts comparable in size to anharmonic constants must be considered. For fluorinated alcohols, where the reduced hydrogen bond strength and enhanced volatility alleviates the intensity problem, we have previously reported supersonic jet overtone data[11,23]. In solution[1], hot bands add to solvent shifts, rendering a quantitative analysis difficult. This leaves the gas phase as the preferred environment for such studies, although the more weakly interacting matrices of Ne and p-H_2 are also attractive due to the much longer interaction times of photons with individual molecules.

The fundamental OH stretching spectrum of methanol[8], ethanol[24] and *t*-butyl alcohol[25] dimers is well characterized, whereas no information on any of their OH stretching overtones is available in the gas phase literature. The only indirect evidence is from an isotopic shift analysis after deuteration[8,10,24], but as we will show, this analysis can be misleading. The purpose of the present work is thus to provide rigorous experimental benchmarks for the diagonal anharmonicity in the OH stretching mode of hydrogen-bonded alcohols to be compared with perturbation theory[12,21,26–30] and variational[31,32] as well as isolated 1-dimensional[33,34] treatments based on quantum-chemical potential energy hypersurfaces[35].

2 Experimental

Methanol (VWR, 99.9%), ethanol (Roth, $\geq$99.8%) and *t*-butyl alcohol (Roth, $\geq$99%) were used as purchased. After flowing through the liquid substances in cooled saturators, helium (Linde, 99.996%) was filled into the gas reservoir of the *filet*-jet, previously described in detail[23]. The mixtures were further diluted with helium through a second inlet and co-addition of argon (Air Liquide, 99.998%) could be realized via a third valve. The concentration of the alcohols in helium was estimated from their vapor pressures, the argon concentration by measuring its flow velocity. A long aspect ratio (*fi*ne but *le*ng*th*y) slit nozzle (600 x 0.2 mm^2) was employed to expand the samples into a continuously pumped (2500 m^3/h) vacuum (<1 mbar) chamber (23 m^3). 180 ms gas pulses were synchronized to the 60 kHz 2 cm^{-1} resolution scans of a Bruker IFS 66v/S FTIR spectrometer. The transmission range of CaF_2 optics covered all spectral regions of interest. A 2 mm InSb detector was employed to measure the fundamental and overtone regions at the same time, providing approximate intensity comparisons for the monomer transitions in the jet expansion. While the InSb detector was sufficient to detect all species in the OH fundamental region, a 3 mm InGaAs detector together with a bandpass filter was used for increased sensitivity in the overtone region, enabling the detection of weak dimer signals. A correction factor was deduced from comparing monomer overtone intensities in the InSb and InGaAs overtone spectra, enabling the evaluation of the dimer intensity ratio from both spectral regions. Due to the weakness of overtone transitions, spectra from more than 1000 gas pulses had to be coadded in the respective range, whereas single gas pulses can produce alcohol dimer donor bands with a signal-to-noise ratio in excess of 20 in the fundamental range if suitable bandpass filters are employed.

Band intensities were obtained by integration of the absorbance spectra using two different integration routines. In case of overlapping bands, the spectra had to be fitted for this purpose. Because the jet spectra are not pressure-broadened beyond the employed instrumental resolution of 2 cm^{-1}, monomer integrations could be affected by sizeable errors. In particular at high absorbance, this error could easily

reach a factor of 2. For dimers, the small rotational constants and homogeneous broadening increase our confidence in relative integrated intensities.

The high resolution spectrum of 10 mbar ethanol in 1 bar N_2 was measured in a 23 cm gas cell with a Bruker Vertex 70V spectrometer at 0.35 cm^{-1} resolution. Errors for all measured spectroscopic constants have been estimated and are given in parenthesis, thus 1.0(1) means 1±0.1 and 1000(100) means 1000±100.

To complement the jet data, two matrix isolation experiments were carried out on methanol dimers in the NCTU laboratory. A gold-plated copper block, cooled with a closed-cycle refrigerator system (Janis RDK-415), served as both a substrate for the matrix sample and a mirror to reflect the incident IR beam to the detector. A gaseous mixture of CH_3OH/*p*-H_2 (1/150, flow rate 35 mmol h^{-1}) was deposited at 3.2 K for 6 h, whereas a gaseous mixture of CH_3OH/Ne (1/150, flow rate 11 mmol h^{-1}) was deposited at 5.0 K for 26 h and cooled to 3.2 K. IR absorption spectra were recorded with a FTIR spectrometer (Bomem, DA8) equipped with a quartz-halogen lamp, CaF_2 beamsplitter and an InSb detector that was cooled to 77 K to cover the spectral range 2000-7500 cm^{-1}. Typically 600 scans at resolution 0.10 cm^{-1} were recorded after each step of deposition for 1.0-1.5 h.

Methanol (J. T. Baker, Absolute Grade) and Ne (99.999%, Scott Specialty Gases) were used as purchased. Normal H_2 (99.9999%, Scott Specialty Gases) was passed through a trap at 77 K before entering a copper cell, filled with hydrous iron (III) oxide catalyst (Aldrich) and cooled to 12.6 K with a closed-cycle refrigerator (Advanced Research Systems, DE204AF), for *p*-H_2 conversion. After conversion, the concentration of *o*-H_2 is less than 10 ppm according to the Boltzmann distribution.

3 Results

3.1 Methanol

The OH band centers and anharmonicity constant of methanol monomer are actually not straightforward to extract from the spectra due to strong rovibrational couplings and torsional tunneling[36]. For the fundamental, we use the value of 3686 cm^{-1} derived from jet-cooled FTIR and Raman band maxima[8], but one can also argue using the high resolution band center near 3685 cm^{-1} [36] or even a torsion-decoupled, but model-dependent value of 3678 cm^{-1} [36]. For the overtone, we use the jet FTIR band maximum of the centre band at 7198 cm^{-1} from the present work (see Fig 1), but one can again argue using the average over the A/E torsional states of 7196 cm^{-1} [37] or an approximately torsion-decoupled value of 7185 cm^{-1} [36,38]. For the corresponding pairings, the resulting anharmonic constant $x_{OH,OH}$ is $-87\,cm^{-1}$, $-87\,cm^{-1}$, and $-85.5\,cm^{-1}$, respectively. A value of $-86(1)\,cm^{-1}$ for $x_{OH,OH}$ thus appears to be robust and also agrees with a fit involving several vibrational states[37]. To judge the performance of the much more sensitive matrix isolation technique[10], one may note that the methanol stretching transitions are N_2-matrix-shifted by $-22\,cm^{-1}$ (fundamental) and $-39\,cm^{-1}$ (overtone), whereas the anharmonic constant is only reduced by 1-2 cm^{-1} compared to the gas phase. For Ar-matrices, the corresponding numbers are slightly closer to our gas phase values[10]. This is even more true for the *p*-H_2 matrix spectra reported in Fig. 2, where the overtone shift amounts to about $-27\,cm^{-1}$. In Ne matrices[39] (see Fig. 3), there is actually a small blue shift of $+9\,cm^{-1}$ for the overtone. In both cases, the anharmonicity constant $x_{OH,OH} = -86\,cm^{-1}$ is identical to the gas phase value within its error margins. This indicates that the matrix isolation approach affects monomer harmonic and anharmonic constants in the sub-% range with particularly small effects for Ar, *p*-H_2 and Ne. The same is true for the isotopic shift analysis of methanol and methanol-OD[8], which yields $x_{OH,OH}$=−87 cm^{-1}.

We will now address the question whether this also holds for methanol dimer. Fig. 1 shows the OH stretching overtone spectrum obtained from a 0.5% methanol expansion in 0.8 bar helium, superimposed on the corresponding fundamental spectrum recorded under exactly the same conditions. The

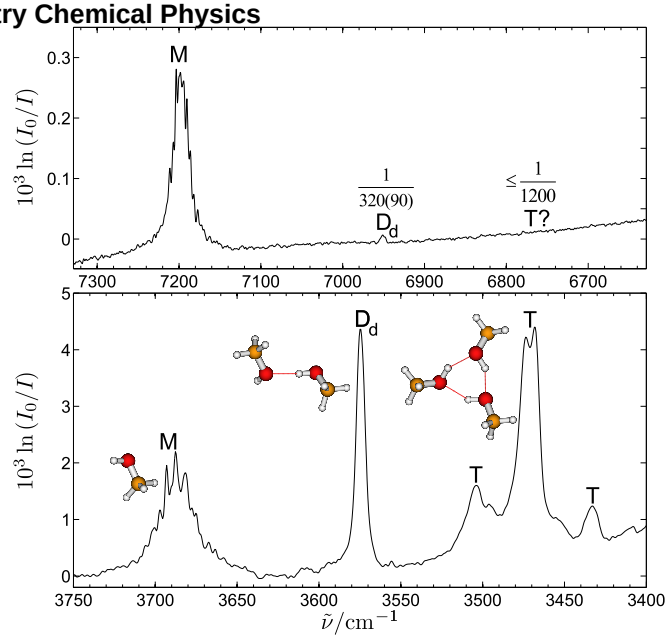

Fig. 1 Fundamental (200 pulses) and overtone (1450 pulses) spectra of 0.5% methanol in 0.8 bar helium expansions. Intensity ratios of overtone to fundamental bands are given as fractions. The broad monomer (M) bands bury the signals of the hydrogen bond acceptor of the dimer. The dimer donor band (D_d) is visible in both spectra, whereas trimer (T) signals are not observed in the overtone region.

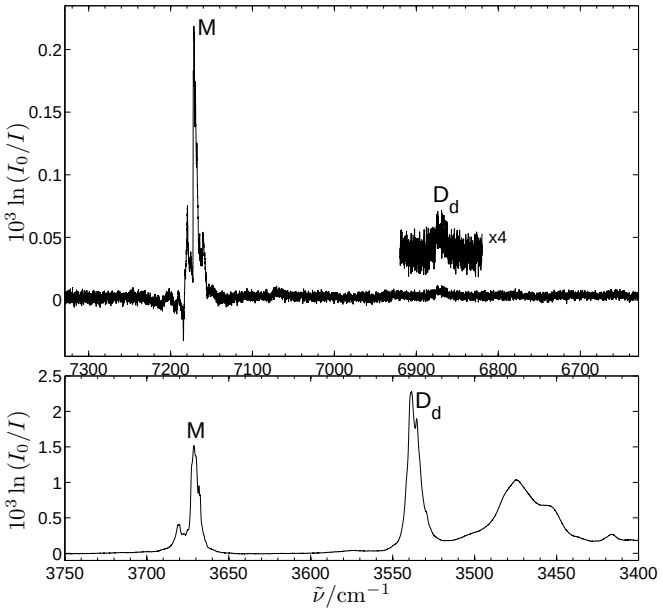

Fig. 2 Fundamental and overtone partial IR spectra of a $CH_3OH/p\text{-}H_2$ (1/150) matrix after deposition at 3.2 K for 1.5 h.

two spectral windows are positioned such that the monomer transitions match and the overtone spectrum is compressed by exactly a factor of 2, such that any change in the dimer anharmonicity constant relative to the monomer value is graphically reflected by a shift of the corresponding dimer transition. Only one very weak dimer overtone transition is seen in the jet spectrum (D_d), further shifted from the monomer than the corresponding strong fundamental transition. It corresponds to the hydrogen-bonded OH, whereas the free OH band in the dimer is buried in the complex rovibrational pattern of the monomer (M). The position of the single dimer donor band is 6950.6(6) cm^{-1}. In combination with the fundamental band position at 3574.5(3) cm^{-1}, an anharmonicity constant of $-99.2(4)\,cm^{-1}$ is obtained. In an N_2 matrix, three transitions at 6833, 6800 and 6764 cm^{-1} are observed[10]. This complex pattern reflects the observation in the fundamental region and is attributed to different dimer conformations or packing effects in the matrix, to which the OH stretching frequency reacts very sensitively. Because of the parallelism of fundamental and overtone perturbations, it is still possible to extract an anharmonicity constant for each of these sites. It amounts to $-105\,cm^{-1}$ for the dominant matrix signal. Hence, the anharmonicity increases by about 15% in the gas phase from the methanol monomer to the dimer and by about 24% in the matrix. The reason is most likely a cooperative $OH\cdots OH\cdots N_2$ hydrogen bond pattern in the matrix, which weakens the donor OH bond more than if the acceptor has no binding partner. Therefore, a nitrogen matrix is too reactive to study isolated hydrogen-bond-induced anharmonicities in a quantitative way, but the qualitative agreement is still satisfactory. We should mention that the analysis of Ar matrix spectra ($-102.5\,cm^{-1}$)[10] leads to better agreement with the gas phase anharmonicity. This trend continues for the data presented in Figs. 2 and 3 for $p\text{-}H_2$ ($-102\,cm^{-1}$) and Ne (-96 to $-98\,cm^{-1}$) matrices. The advantage of the former is that site splittings are largely absent, whereas the latter matrix is somewhat closer to the gas phase value, approaching it from the other side. Less satisfactory is the deuterium isotope analysis of the donor vibration[8], which has led to an estimated methanol dimer donor anharmonicity constant of just $-89\,cm^{-1}$. This is only 2% larger than the monomer value in the same analysis, whereas the correct answer is 15%. Hence, there is a large range of previously estimated anharmonicity increases in methanol-OH upon dimerization, ranging from 2% to 24%. The present experiment settles this order-of-magnitude range more or less in between, at 15(1)%.

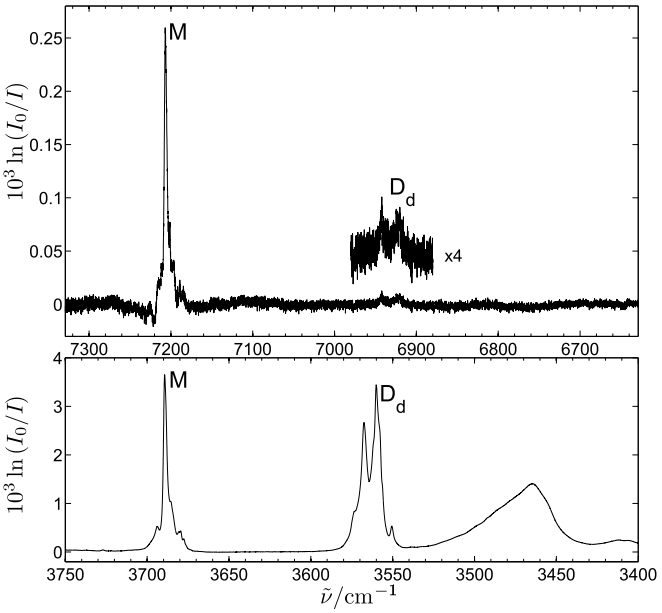

Fig. 3 Fundamental and overtone partial IR spectra of a CH_3OH/Ne (1/150) matrix after deposition at 5.0 K for 4.5 h.

An advantage of the matrix approach is that even the acceptor OH can be separated from the sharp monomer transition, although with similar site splitting effects. The corresponding anharmonicity constants are observed[10] to be within 1 cm^{-1} of the monomer values for N_2 and Ar matrices, as expected. However, the position of the acceptor bands shifts from 0.4% lower than the monomer in N_2 to 0.4% higher than the monomer in Ar matrices. In the case of $p\text{-}H_2$ and Ne matrices, the acceptor bands are somewhat difficult to identify and will be the subject of a separate study. The available gas

phase evidence is also somewhat contradictory, claiming the acceptor at 3684 [40,41] or 3675 cm^{-1} [21].

The intensity effects on the overtone transition are more dramatic. By integrating the area underneath the dimer bands in Fig. 1, which were measured under identical expansion conditions, one obtains a ratio of 320(90), by which the fundamental is stronger than the dimer overtone. The corresponding published matrix isolation value [10] is 420, independent on the matrix gas and slightly larger than the gas phase value. For the lighter *p*-H_2 and Ne matrices studied in this work, approximate intensity ratios between fundamental and overtone transitions of the hydrogen bonded OH stretching mode of 300(100) and 300(150), respectively, can be extracted from spectra recorded in an early deposition phase, where the fundamental transitions are not yet saturated to a large degree. The 320-fold gas phase enhancement of the fundamental relative to the overtone is to be compared to the corresponding monomer ratio, which is 6(1) in the jet spectra, and between 12 in an Ar matrix, and 20 in a N_2 matrix. Again, the lighter matrices yield somewhat lower values of 9(3) for *p*-H_2 and 11(3) for Ne, likely because they give rise to less hydrogen bond enhancement of the fundamental than Ar and in particular N_2. The strong sensitivity of the monomer intensity ratio to the environment could also be related to the complex coupling pattern in this mode, but a residual integration error cannot be ruled out in our monomer jet spectra due to the low spectral resolution and the sharp monomer transitions. For the room temperature gas phase, where our experimentally estimated monomer ratio of about 6 is particularly problematic due to higher extinction, agreement with the reliable literature value [42] of 12.1(9) is still within a factor of two.

More interesting is the dimer donor/monomer intensity ratio in the two spectral ranges. As we have no experimental way to determine the dimer concentration, we have to rely on a literature reference. Huisken *et al.* [41] determined a ratio of 12.3(6) in the fundamental range, assuming equal dissociation and absorption cross sections. This leads to a dimer donor/monomer intensity ratio of about 0.5 in the overtone range (using the literature fundamental/overtone ratio for the monomer [42]). However, in converting the monomer reference [43], Huisken *et al.* [41] may have overlooked an lg/ln conversion. Therefore, a more realistic overtone dimer donor/monomer intensity ratio may be closer to 1, but we emphasize that this ratio is outside our own experimental evidence. In summary, the order of magnitude overtone attenuation of infrared intensity in methanol monomer changes to a 320-fold attenuation in the hydrogen-bonded dimer OH and the order of magnitude intensity enhancement of the fundamental upon hydrogen bonding is lost in the overtone. This represents a helpful benchmark for anharmonic calculations on multidimensional potential and dipole hypersurfaces.

Adding the methanol dimer acceptor and donor fundamental wavenumbers, we predict their combination band slightly above or - considering the expected negative cross-anharmonicities - even within the band profile of the monomer overtone. Therefore, it is not surprising that it is not observed in our spectra. A remarkable qualitative feature in Fig. 1 is the complete absence of trimer overtone spectral intensity, despite a very sizeable fundamental transition, which has been analyzed before in detail [8]. This absence means that the trimer OH stretching overtones and combinations must be at least three orders of magnitude weaker than the trimer fundamentals, in agreement with the finding by matrix isolation [10] (see also Figs. 2 and 3).

3.2 *t*-Butyl alcohol

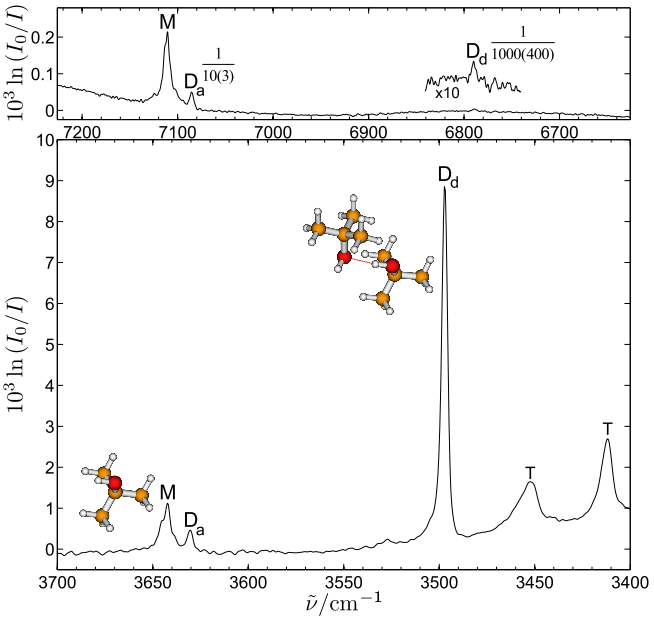

Fig. 4 Fundamental (200 pulses) and overtone (1350 pulses) spectra of 0.3% *t*-butyl alcohol in 0.8 bar helium expansions. Intensity ratios of overtone to fundamental bands are given as fractions. The monomer (M) bands feature some rotational structure. The intensity of the bands of the dimer acceptor (D_a) and donor (D_d) are affected differently by the hydrogen bond.

When moving from methanol to *t*-butyl alcohol, the electron-donating methyl groups improve the hydrogen bond acceptor character of the alcohol, and to a lesser extent probably also its donor quality [44]. This strengthens the hydrogen bond and results in an increased red-shift of the OH group frequency. Fig. 4 shows the corresponding fundamental [25] and overtone spectra in the style of Fig. 1 and the determined wavenumbers are given in Tab. 1. Due to the smaller rotational constants, the monomer (M) signals are narrower (although rotational branches are still visible) and allow for the

detection of the weakly red-shifted acceptor OH mode of the dimer (D_a). The shift is similar to that of methanol[21] (unless one adopts the earlier assignments[40,41]) and the anharmonicity constant ($-87.9(3)\,cm^{-1}$) is indeed very close to that of the monomer ($-87.0(2)\,cm^{-1}$). The monomer anharmonicity constant was previously determined with larger uncertainty from fits to several room temperature gas phase overtones[42,45]. The small difference between monomer and dimer acceptor leads to the conclusion that free OH groups hardly sense the electron-donating effect of the three additional methyl groups. The opposite is the case for the donor OH vibration (D_d). It is now red-shifted by $145.2(4)\,cm^{-1}$ from the monomer, about 30% more than for methanol. The anharmonic constant ($-102.6(4)\,cm^{-1}$) now exeeds that of the monomer by about 18%, compared to ∼15% for methanol. These trends are subtle compared to the intensity effects. The fundamental/overtone ratio is 4(1) in the jet-cooled monomer, lower than the literature gas phase value of 6.8(8)[42]. It increases to 10(3) in the acceptor band and to 1000(400) in the donor band of the dimer. This demonstrates the sensitivity of OH overtone intensities to the hydrogen bond strength, which exceeds that of the wavenumber shift by at least an order of magnitude. The intensity ratio for the trimer transitions is expected to be higher than a factor of 800, which we derive as a lower bound. This lower bound is comparable to the dimer donor ratio, just because the trimer fundamental is less intense in our jet spectra than in the case of methanol.

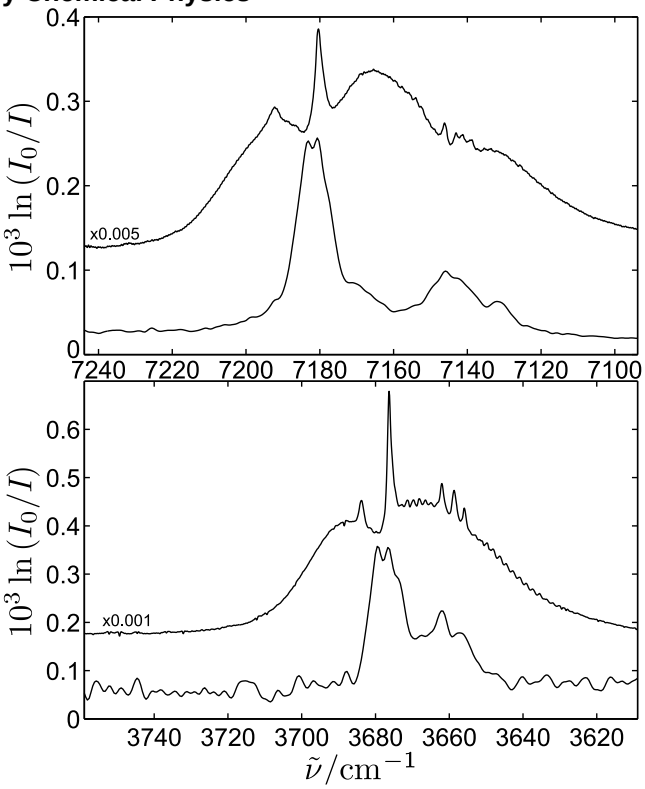

Fig. 5 Comparison of gas phase (upper trace, $0.35\,cm^{-1}$ resolution) with jet spectra of ethanol (lower trace, $2\,cm^{-1}$ resolution, fundamental: 0.3 bar helium, 0.1% ethanol; overtone: 0.9 bar helium, 0.3% ethanol)

Table 1 Measured band centres of *t*-butyl alcohol monomer (M), dimer acceptor (D_a) and donor (D_d) OH stretching vibrations in cm^{-1}

	M	D_a	D_d
$\tilde{\nu}_{OH}$	3642.3(2)	3630.4(2)	3497.1(3)
$2\tilde{\nu}_{OH}$	7110.6(2)	7085.1(4)	6789.1(4)

3.3 Ethanol

Ethanol represents an intermediate case between methanol and *t*-butyl alcohol in terms of hydrogen bond acceptor quality[44]. Its spectra are complicated by the fact that the monomer intensity is distributed among two conformers (gauche and trans). Figure 5 shows the ethanol monomer OH stretching fundamentals and overtones in the room temperature gas phase at higher resolution ($0.35\,cm^{-1}$) and in jet expansions at lower resolution ($2\,cm^{-1}$). We find the fundamental OH stretching wavenumbers of the trans conformer at $3676.6(2)\,cm^{-1}$ and the overtone transition at $7180.6(2)\,cm^{-1}$ in the jet, resulting in an anharmonicity constant of $-86.3(2)\,cm^{-1}$. It compares well to a literature value of 85.0(4) from averaging over several overtone transitions of trans ethanol in the gas phase[46]. The OH stretching bands of the trans conformer show some rotational structure in the jet expansion. The gauche monomer vibrational states are split into an upper (u) and lower (l) level due to the tunneling motion between the two enantiomeric gauche forms. This fact, combined with the low resolution and overlap with acceptor bands of dimers renders the assignment of gauche ethanol in the jet spectrum difficult. However, in the room temperature gas phase spectrum, three prominent peaks can be observed among a rich rotational/hot band structure at the fundamental OH stretching position. We assign the highest energy peak at $3662.0(1)\,cm^{-1}$ to the $l \rightarrow u$ transition and the lowest energy peak at $3655.9(1)\,cm^{-1}$ to the $u \rightarrow l$ transition. Given the ground state splitting of $3.3\,cm^{-1}$[47] the $u \rightarrow u$ and $l \rightarrow l$ transition can be expected at $3658.7\,cm^{-1}$ and $3659.2\,cm^{-1}$, respectively. They may both overlap in the observed peak at $3658.7(1)\,cm^{-1}$ and correspond to the Raman transition observed at $3660\,cm^{-1}$[24]. From this data, a decreased tunneling splitting of $2.8(1)\,cm^{-1}$ can be derived for the first excited OH stretching state. From the above wavenumbers the band center of the fundamental would be at $3659.0(1)\,cm^{-1}$. However, the true centers of the peaks can be expected to be somewhat blue-shifted, as is also apparent

from the comparison with the cold jet spectra. Therefore we expect the band center of the gauche ethanol fundamental at 3659.3(4). Until a high resolution verification, these plausible assignments must remain tentative. For the overtone four features are found in the gauche region. The highest energy band at 7146.2(2) cm^{-1} is clearly separated from the others and can be assigned to the (l → u) transition. The other three features are partly overlapping, but the (u → u) transition can be expected at 7142.9 cm^{-1} and is assigned to the band at 7143.1(1) cm^{-1}, given the 3.3 cm^{-1} ground state splitting[47]. For the other two bands we see two possibilities of assignment: a) Assigning the lowest energy band at 7139.0(4) cm^{-1} to the (u → l) transition would lead to an expected band position for (l → l) at 7142.3 cm^{-1}, which fits with the band at 7141.5(3) cm^{-1} rather poorly. b) Disregarding the lowest energy band and assigning the (u → l) transition to the neighbouring band at 7141.5(3) cm^{-1} leads to an expected band position for (l → l) at 7144.8, where no band is observed at all in the spectrum.

Neither interpretation provides a satisfying assignment for the (l → l) transition. Also, b) does not include the feature at 7139.0(4) cm^{-1}, but it would fit better the expectation of a further decreasing tunneling splitting; 1.5(3) cm^{-1} for v = 2. Possibility a) leads to an increased tunneling splitting of 4.0(3) cm^{-1} – even higher than for the ground state, but possible in case of interactions with other vibrational levels. The anharmonicity constants can be derived from averaging over the respective tunneling transitions (again acknowledging the possible thermal shift) and amount to $-87.9(5)\,cm^{-1}$ for a) (band center at 7142.9(7)) and to $-87.2(6)\,cm^{-1}$ for b) (band center at 7144.2(8)). While a safe assignment of the gauche OH stretching overtone bands definitely requires a rotationally resolved spectrum, its anharmonicity constant is likely within the $-88(1)\,cm^{-1}$ interval, which we adopt in the following. Again, it is in good agreement with the literature value of 86(1) from averaging over several overtone transitions of gauche ethanol in the gas phase[46]. The observed gas phase bands are seen in the jet spectrum as broad features overlapping with each other and with the dimer acceptor vibrations. However, the intensity ratios between the fundamentals and the overtones can be estimated from curve fitting the jet spectra at identical expansion conditions to be 5(1) for trans and 5(2) for gauche ethanol monomer, again lower than the gas phase average over all conformers of 7.5(4)[42].

There are at least four distinguishable dimer conformations in helium expansions of ethanol[24]. This makes the detection of the corresponding dimer overtones very challenging (see Fig. 6). We succeeded by adding a trace of Ar as a relaxation promotor which favors the global minimum structure of the dimer[24], a homochiral double-gauche structure with weakly attractive secondary C-H···O contacts. By collecting most of the dimers in this conformation, a very weak donor

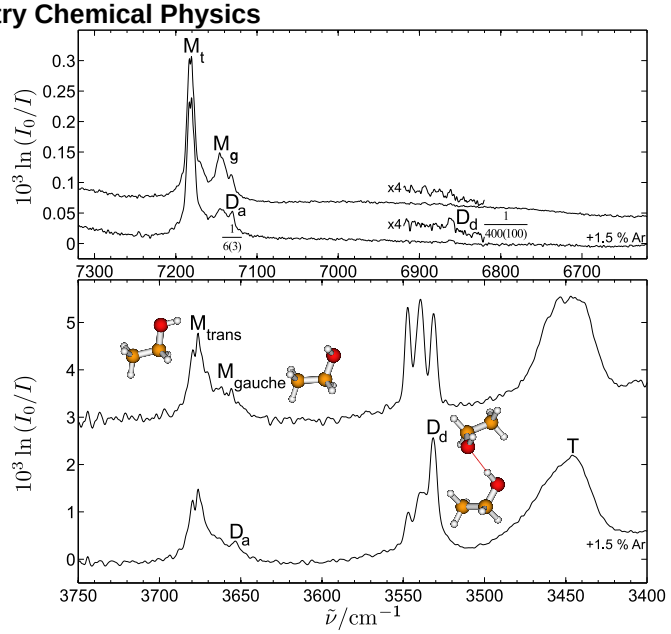

Fig. 6 Spectra of 0.3% ethanol in 0.9 bar expansions in the fundamental (upper: pure helium, 100 scans; lower: helium + 1.5% argon, 200 scans) and overtone range (upper: pure helium, 3450 scans; lower: helium + 1.5% argon, 1600 scans) Intensity ratios of overtone to fundamental bands are given as fractions. The trans monomer (M_{trans}) bands feature some rotational structure, whereas the gauche monomer bands (M_{gauche}) coincide with dimer acceptor bands. The population of the most stable dimer is increased upon co-addition of argon, thus the overtone of its donor D_d vibration becomes enhanced and visible in the spectrum, whereas its acceptor band D_a can be distinguished more clearly from transitions of other species.

overtone band becomes visible at 6860.9(7) cm^{-1}. The corresponding fundamental is at 3531.5(2) cm^{-1}. This makes the donor vibration intermediate in its hydrogen-bonded fundamental red-shift from the monomer (127.8(4) cm^{-1}), its anharmonicity constant ($-101.1(4)\,cm^{-1}$) and its overtone intensity loss (400(100)-fold) between methanol and *t*-butyl alcohol, as one would expect. In the expansion of ethanol with pure helium one may optimistically try to assign dimer donor bands to features of a signal to noise ratio near to unity. This leads to large error bars for the spectroscopic constants, as can be seen for the donor vibration in the most stable dimer giving $x_{OH,OH} = -101(1)\,cm^{-1}$ and an intensity ratio of 400(200). For the donor of the second most stable dimer which was attributed to the fundamental at 3547.1(3)[24] this would give an anharmonicity of $-100.2(6)\,cm^{-1}$ and a fundamental/overtone intensity ratio of 400(200), when a weak feature at 6894(1) cm^{-1} is assigned to it. Other conformers of ethanol dimer contribute to the fundamental signal at 3539.4(3) cm^{-1} [24] and their overtone transitions may be found

in the 6879(3) cm^{-1} region. Again, trimer overtone bands are not observed and should have a fundamental/overtone intensity ratio of at least 800.

The Ar relaxation also makes the dimer acceptor OH fundamental and overtone transitions visible, although their intensity is difficult to quantify. The gauche acceptor of the most stable dimer has been assigned at 3654 cm^{-1} and the trans acceptor of the second minimum structure at 3672 cm^{-1} [24]. We find the gauche acceptor bands at 3653.3(5) cm^{-1} and 7130.3(7) cm^{-1}. They feature slightly increased values both for the anharmonicity of $-88.2(6)$ cm^{-1} and for the fundamental/overtone intensity ratio of 6(3), relative to the monomer. The trans acceptor bands of the second most stable dimer appear as a shoulder on the trans monomer bands at 3670.4(4) cm^{-1} and 7170(2) cm^{-1} in the He expansion without addition of Ar. Within error bars, the trans acceptor anharmonicity constant agrees with that of the trans monomer. However, it seems to have an increased intensity ratio of 8(4). Again, anharmonicity constants from an OD-analysis prove to be unsatisfying, especially for the dimer donor [24].

4 Discussion and Conclusions

Table 2 compares the subtle overtone trends with alkylation, among which the intensity trend is the most pronounced, despite being the least precise experimental quantity listed in the table. We can now firmly state that an alcoholic OH···OH hydrogen bond increases the donor OH anharmonicity constant by 15-18%, whereas even the subtle cooperativity in a nitrogen matrix raises this anharmonicity enhancement well above 20%. Due to the accompanying dramatic loss in intensity, it is not possible to follow this alkylation trend up to trimers or larger oligomers. Even the weakest hydrogen bonds [11,23] are able to double the fundamental/overtone intensity ratio. Regular hydrogen bonds lead to an increase by about one to two orders of magnitude and it can be safely concluded that cooperative hydrogen bonds in trimers, even subject to ring-strain, increase the fundamental/overtone ratio by two orders of magnitude or more.

Table 2 Overtone data on the alcohol dimer donor OH stretching vibrations (from left to right): diagonal anharmonicity constant in cm^{-1}, relative increase of anharmonicity compared to the monomer and decrease of overtone intensity compared to the fundamental transition. The errors of the values are given in parentheses

	$x^{D_d}_{OH,OH}$	$\frac{x^{D_d}_{OH,OH}}{x^{M}_{OH,OH}}$	$\frac{\int_{\nu_{02}} \ln\left(\frac{I_0}{I_{D_d}}\right) d\tilde{\nu}}{\int_{\nu_{01}} \ln\left(\frac{I_0}{I_{D_d}}\right) d\tilde{\nu}}$
Methanol	−99.2(4)	1.15(1)	0.0031(9)
Ethanol	−101.1(4)	1.15(1)	0.0024(7)
t-Butyl alcohol	−102.6(4)	1.179(5)	0.0010(4)

The effect of fluorination [11,23] can now be assessed. The electron-withdrawing effect of the fluorine leads to a slight decrease in anharmonicity in the monomer and also in the dimer. Monomer and dimer acceptor overtones are weaker than in non-fluorinated compounds, relative to the corresponding fundamentals, due to subtle OH···F interactions. The intensity effect in the donor OH bands is not significantly enhanced. It would be interesting to study overtones of weak intramolecular OH hydrogen bonds with our technique. Such systems have been studied before with much more sensitive techniques in the room temperature gas phase [48], but it could be instructive to see how much jet cooling affects the band centers and band intensities. For strong intramolecular hydrogen bonds such as in diols [49], a heated nozzle will probably be required because the associated compounds are typically not very volatile. A disadvantage of such intramolecular hydrogen bonds is that one typically cannot compare in a direct way to the non-hydrogen-bonded reference. Non-resonant UV ionization of laser-excited overtones has the potential of a much higher sensitivity also for non-aromatic alcohols [50]. So far, it seems to have been applied predominantly to aromatic monomers [51], but not to non-aromatic alcohol dimers. An advantage is that the high sensitivity makes higher overtones easily accessible, whereas the present technique is currently limited to second overtones of monomers. Smaller molecules and clusters definitely profit from higher resolution [52], but the 2 cm^{-1} resolution employed in this work is sufficient for the alcohol dimers due to their fast vibrational redistribution and high density of states.

Matrix isolation techniques are seen to be quite reliable in the determination of overtone intensity and frequency effects in alcohol dimers, although one must expect some overestimation of the dimer anharmonicity in strongly perturbing matrices and one must be able to correlate site splittings in the two spectral ranges, which can be of the same order of magnitude as the anharmonicity constants. Site splittings can be minimized in *p*-H_2, whereas Ne provides the smallest shifts from the gas phase, often with opposite sign of those in Ar or N_2. Due to their much higher sensitivity, these matrix isolation techniques are broadly applicable, but it was important to validate their results in the present vacuum isolation approach, before using them to judge the performance of theoretical methods which typically do not include the effect of an environment.

This brings us to the key motivation of the present work, namely to assess the reliability of approximate anharmonic treatments for hydrogen bond-induced changes in the frequency and intensity of OH stretching vibrations. Full-dimensional variational treatments are still out of reach for alcohol dimers. By concentrating on the diagonal anharmonicity effect, 1-dimensional treatments [33,34] may already be useful. However, they cannot predict the anharmonic hydrogen bond-

induced red-shift of the fundamental vibration, as we will see. For this, second-order perturbation theory appears to be the simplest approach with some promise[26]. Therefore, we provide a few exploratory results based on the latter in the ESI†, using the recent implementation by the Barone group[27,28].

In summary, these results indicate that the intensity ratios and OH anharmonicity trends are captured quite satisfactorily. However, the OH stretching frequency shift upon dimerization is clearly and consistently overestimated. This is even more pronounced in the harmonic approximation, but perturbative inclusion of anharmonicity still does not recover the experimental results. To fully understand whether the systematic failure of vibrational perturbation theory to reproduce the experimental OH vibrational hydrogen bond shift in methanol dimer is due to residual electronic structure deficiencies[33], or due to the perturbational treatment of the coupling between the OH stretching mode and hydrogen bond librations (or both), the latter should be characterized experimentally for this prototype system in the far infrared region. Work towards this goal is under way. For the time being, we have experimentally shown that vibrational perturbation theory is quite reliable in describing the increase in (diagonal) OH bond anharmonicity due to hydrogen bonding in alcohol dimers. For the decrease in overtone infrared intensity, this is at least qualitatively the case. All this has been anticipated by Sándorfy[1].

Acknowledgements This work has been supported by the Deutsche Forschungsgemeinschaft (DFG, Grant Su121/4), Ministry of Science and Technology, Taiwan (Grant NSC102-2745-M009-001-ASP), and the Ministry of Education, Taiwan ("Aim for the Top University Plan" of National Chiao Tung University).

References

1 C. Sándorfy, Journal of Molecular Structure, 2006, **790**, 50 – 54.
2 M. Fárník, M. Weimann and M. A. Suhm, The Journal of Chemical Physics, 2003, **118**, 10120–10136.
3 A. Gutberlet, G. Schwaab, Ö. Birer, M. Masia, A. Kaczmarek, H. Forbert, M. Havenith and D. Marx, Science, 2009, **324**, 1545–1548.
4 S. D. Flynn, D. Skvortsov, A. M. Morrison, T. Liang, M. Yong Choi, G. E. Douberly and A. F. Vilesov, The Journal of Physical Chemistry Letters, 2010, **1**, 2233–2238.
5 M. Letzner, S. Gruen, D. Habig, K. Hanke, T. Endres, P. Nieto, G. Schwaab, L. Walewski, M. Wollenhaupt, H. Forbert, D. Marx and M. Havenith, The Journal of Chemical Physics, 2013, **139**, 154304.
6 R. Jiang and E. L. Sibert III, The Journal of Chemical Physics, 2012, **136**, 224104.
7 V. Cervetto, J. Helbing, J. Bredenbeck and P. Hamm, The Journal of Chemical Physics, 2004, **121**, 5935–5942.
8 R. Wugt Larsen, P. Zielke and M. A. Suhm, The Journal of Chemical Physics, 2007, **126**, 194307.
9 J. Liévin, M. A. Temsamani, P. Gaspard and M. Herman, Chemical Physics, 1995, **190**, 419 – 445.
10 J. Perchard and Z. Mielke, Chemical Physics, 2001, **264**, 221 – 234.
11 T. Scharge, D. Luckhaus and M. A. Suhm, Chemical Physics, 2008, **346**, 167 – 175.
12 T. Di Paolo, C. Bourdéron and C. Sandorfy, Canadian Journal of Chemistry, 1972, **50**, 3161–3166.
13 G. E. Hilbert, O. R. Wulf, S. B. Hendricks and U. Liddel, Journal of the American Chemical Society, 1936, **58**, 548–555 and references cited therein.
14 K. Didriche, T. Földes, C. Lauzin, D. Golebiowski, J. Liévin and M. Herman, Molecular Physics, 2012, **110**, 2781–2796.
15 S. A. Nizkorodov, M. Ziemkiewicz, D. J. Nesbitt and A. E. W. Knight, The Journal of Chemical Physics, 2005, **122**, 194316.
16 M. A. Suhm, Advances in Chemical Physics, 2009, **142**, 1–57.
17 M. Umer and K. Leonhard, The Journal of Physical Chemistry A, 2013, **117**, 1569–1582.
18 R. L. Rowley, C. M. Tracy and T. A. Pakkanen, The Journal of Chemical Physics, 2007, **127**, 025101.
19 V. Dyczmons, The Journal of Physical Chemistry A, 2004, **108**, 2080–2086.
20 H. B. Fu, Y. J. Hu and E. R. Bernstein, The Journal of Chemical Physics, 2006, **124**, 024302.
21 H.-L. Han, C. Camacho, H. A. Witek and Y.-P. Lee, The Journal of Chemical Physics, 2011, **134**, 144309.
22 I. León, R. Montero, A. Longarte and J. A. Fernández, The Journal of Chemical Physics, 2013, **139**, 174312.
23 M. A. Suhm and F. Kollipost, Phys. Chem. Chem. Phys., 2013, **15**, 10702–10721.
24 T. N. Wassermann and M. A. Suhm, The Journal of Physical Chemistry A, 2010, **114**, 8223–8233.
25 D. Zimmermann, T. Häber, H. Schaal and M. A. Suhm, Molecular Physics, 2001, **99**, 413–425.
26 G. Amat, H. Nielsen and G. Tarrago, Rotation-Vibration Spectra of Molecules, M. Dekker, New York, 1971.
27 V. Barone, The Journal of Chemical Physics, 2005, **122**, 014108.
28 J. Bloino and V. Barone, The Journal of Chemical Physics, 2012, **136**, 124108.
29 C. Emmeluth, V. Dyczmons, T. Kinzel, P. Botschwina, M. A. Suhm and M. Yanez, Phys. Chem. Chem. Phys., 2005, **7**, 991–997.
30 H. G. Kjaergaard, A. L. Garden, G. M. Chaban, R. B. Gerber, D. A. Matthews and J. F. Stanton, The Journal of Physical Chemistry A, 2008, **112**, 4324–4335.
31 J. M. Bowman, T. Carrington and H.-D. Meyer, Molecular Physics, 2008, **106**, 2145–2182.
32 F. Pfeiffer and G. Rauhut, The Journal of Chemical Physics, 2014, **140**, 064110.
33 A. Bleiber and J. Sauer, Chemical Physics Letters, 1995, **238**, 243 – 252.
34 R. Vianello, B. Kovačević, G. Ambrožič, J. Mavri and Z. B. Maksić, Chemical Physics Letters, 2004, **400**, 117 – 121.
35 J. M. Bowman, X. Huang, N. C. Handy and S. Carter, The Journal of Physical Chemistry A, 2007, **111**, 7317–7321.
36 R. Hunt, W. Shelton, F. A. Flaherty and W. Cook, Journal of Molecular Spectroscopy, 1998, **192**, 277 – 293.
37 D. Rueda, O. V. Boyarkin, T. R. Rizzo, A. Chirokolava and D. S. Perry, The Journal of Chemical Physics, 2005, **122**, 044314.
38 D. Rueda, O. V. Boyarkin, T. R. Rizzo, I. Mukhopadhyay and D. S. Perry, The Journal of Chemical Physics, 2002, **116**, 91–100.
39 J. Perchard, F. Romain and Y. Bouteiller, Chemical Physics, 2008, **343**, 35 – 46.
40 R. A. Provencal, J. B. Paul, K. Roth, C. Chapo, R. N. Casaes, R. J. Saykally, G. S. Tschumper and H. F. Schaefer III, The Journal of Chemical Physics, 1999, **110**, 4258–4267.
41 F. Huisken, A. Kulcke, C. Laush and J. M. Lisy, The Journal of Chemical Physics, 1991, **95**, 3924–3929.
42 K. R. Lange, N. P. Wells, K. S. Plegge and J. A. Phillips, The Journal of Physical Chemistry A, 2001, **105**, 3481–3486.

43 R. G. Inskeep, J. M. Kelliher, P. E. McMahon and B. G. Somers, The Journal of Chemical Physics, 1958, **28**, 1033–1036.

44 C. Emmeluth, V. Dyczmons and M. A. Suhm, The Journal of Physical Chemistry A, 2006, **110**, 2906–2915.

45 H. L. Fang and D. A. C. Compton, The Journal of Physical Chemistry, 1988, **92**, 6518–6527.

46 H. L. Fang and R. L. Swofford, Chemical Physics Letters, 1984, **105**, 5 – 11.

47 J. C. Pearson, C. S. Brauer and B. J. Drouin, Journal of Molecular Spectroscopy, 2008, **251**, 394 – 409.

48 B. J. Miller, J. R. Lane and H. G. Kjaergaard, Phys. Chem. Chem. Phys., 2011, **13**, 14183–14193.

49 D. L. Howard and H. G. Kjaergaard, The Journal of Physical Chemistry A, 2006, **110**, 10245–10250.

50 T. Omi, H. Shitomi, N. Sekiya, K. Takazawa and M. Fujii, Chemical Physics Letters, 1996, **252**, 287 – 293.

51 B. J. Miller, H. G. Kjaergaard, K. Hattori, S.-i. Ishiuchi and M. Fujii, Chemical Physics Letters, 2008, **466**, 21 – 26.

52 K. Didriche, C. Lauzin, T. Földes, D. Golebiowski, M. Herman and C. Leforestier, Phys. Chem. Chem. Phys., 2011, **13**, 14010–14018.